Contrib Mineral Petrol (2005) 16: 181–195
DOI 10.1007/s00410-004-0643-6

ORIGINAL PAPER

Matthias Konrad-Schmolke · Mark R. Handy
Jochen Babist · Patrick J. O'Brien

Thermodynamic modelling of diffusion-controlled garnet growth

Received: 16 June 2004 / Accepted: 17 November 2004 / Published online: 13 January 2005

Abstract Numerical thermodynamic modelling of mineral composition and modes for specified pressure-temperature paths reveals the strong influence of fractional garnet crystallisation, as well as water fractionation, on garnet growth histories in high pressure rocks. Disequilibrium element incorporation in garnet due to the development of chemical inhomogeneities around porphyroblasts leads to pronounced episodic growth and may even cause growth interruptions. Discontinuous growth, together with pressure- and temperature-dependent changes in garnet chemistry, cause zonation patterns that are indicative of different degrees of disequilibrium element incorporation. Chemical inhomogeneities in the matrix surrounding garnet porphyroblasts strongly affect garnet growth and lead to compositional discontinuities and steep compositional gradients in the garnet zonation pattern. Further, intergranular diffusion-controlled calcium incorporation can lead to a characteristic rise in grossular and spessartine contents at lower metamorphic conditions. The observation that garnet zonation patterns diagnostic of large and small fractionation effects coexist within the same sample suggests that garnet growth is often controlled by small-scale variations in the bulk rock chemistry. Therefore, the spatial distribution of garnet grains and their zonation patterns, together with numerical growth models of garnet zonation patterns, yield information about the processes limiting garnet growth. These processes include intercrystalline element transport and dissolution of pre-existing grains. Discontinuities in garnet growth induced by limited element supply can mask traces of the thermobarometric history of the rock. Therefore, thermodynamic modelling that considers fractional disequilibrium crystallisation is required to interpret compositional garnet zonation in terms of a quantitative pressure and temperature path of the host rock.

Editorial Responsibility: J. Hoefs

M. Konrad-Schmolke (✉) · M. R. Handy · J. Babist
Geowissenschaften, Freie Universität Berlin, Haus B,
Malteserstrasse 74-100, 12249 Berlin, Germany
E-mail: mkonrad@zedat.fu-berlin.de
Tel.: +49-30-83870339
Fax: +49-30-83870734

P. J. O'Brien
Institut für Geowissenschaften, Universität Potsdam,
Postfach 601553, 14415 Potsdam, Germany

Introduction

Zonation patterns in metamorphic minerals are often used to constrain the pressure–temperature (P–T) path of their host rock (Spear and Selverstone 1983; Menard and Spear 1993; Okadaira 1996; Ayres and Vance 1997; Enami 1998; Cooke et al. 2000; Escuder-Viruete et al. 2000), to determine the duration of metamorphic events (Lasaga and Jiang 1995; Ganguly et al. 1996; Perchuck et al. 1999) and to gain insight into crystal growth and transport mechanisms in metamorphic rocks (Hollister 1966; Loomis and Nimick 1982; Cygan and Lasaga 1982; Chernoff and Carlson 1997; O'Brien 1999; Spear and Daniel 2001). Garnet is suited for these purposes because its composition is very sensitive to pressure and temperature changes, but also because cation diffusion in garnet is sufficiently slow to preserve compositional differences within a grain. The growth zonation pattern in garnet depends on pressure (P), temperature (T), growth rate and also on changes in the chemical composition (X) of the matrix in equilibrium with the garnet surface (Spear 1993; Menard and Spear 1993). Therefore, growth zonation in garnet contains information on all these parameters during growth.

Growth zonation preserved in garnet porphyroblasts is interpreted as evidence for fractional crystallisation, which changed the chemical composition of the matrix around the porphyroblast during growth (Marmo et al. 2002). The chemical composition of the matrix around the porphyroblast depends on the amounts of elements fractionated into the garnet crystal and on the transport

rate of these elements into the matrix volume (Carlson 1989; Chernoff and Carlson 1997). If fractional garnet crystallisation in a given matrix volume is faster than the transport of garnet nutrients into this volume, the composition of the matrix reservoir is progressively depleted in elements fractionated into the garnet crystal. Because these chemical changes are recorded in the zonation pattern, they can be used to determine relative growth-velocities and diffusion-velocities, as well as the mechanisms that control the garnet growth. Intercrystalline transport velocities and growth-controlling mechanisms in natural rocks have been the focus of several papers that deal mainly with porphyroblast nucleation processes (e.g. Carlson 1989; Carlson 1991; Miyazaki 1991; Chernoff and Carlson 1997; Spear and Daniel 2001). Other papers have concentrated on numerical simulations to constrain the complex feedback between matrix chemistry, garnet composition and growth mechanisms (e.g. Loomis and Nimick 1982; Loomis, 1982; Spear 1993; Menard and Spear 1993). These numerical models assume complete chemical equilibrium between the garnet surface and matrix phases throughout the system. However, there is ample evidence that chemical equilibrium, even over small distances, is never attained in many metamorphic rocks. Chernoff and Carlson (1997) and Spear and Daniel (2001) found evidence for disequilibrium incorporation of calcium in garnet due to chemical inhomogeneities and sluggish intercrystalline element transport in metapelitic rocks. Recent studies show that even rapidly diffusing elements such as manganese may have very short length scales of equilibration (Hirsch et al. 2003).

In this paper, we model the effects of fractional garnet crystallisation on the zonation pattern of metamorphic garnets. Further, we assume that garnet growth is controlled by the flux of nutrients to the garnet surface, rather than by chemical equilibrium with other matrix phases. The aim of the study is to interpret commonly observed garnet zonation patterns in order to yield insight into growth processes and transport properties of the rock matrix in the vicinity of garnet.

Thermodynamic modelling of compositional zonation patterns

Equilibrium thermodynamics enable us to calculate mineral assemblages and mineral compositions in a rock with known bulk composition (e.g. Meyre et al. 1997; Powell et al. 1998; Vance and Mahar 1998; Worley and Powell 2000; White et al. 2000, 2001). This method has been used to reconstruct compositional changes of minerals in a given chemical system during metamorphic evolution (e.g. Spear et al. 1984; Vance and Mahar 1998). In the following, we calculate pseudosections and garnet zonation patterns with a Gibbs energy minimisation approach, using the software package THERIAK-DOMINO of de Capitani and Brown (1986) and the internally consistent dataset of Holland and Powell (1998). The solution models used in the calculations are given in Appendix 2.

We distinguish three different types of garnet crystallisation: (1) homogeneous equilibrium crystallisation, where all phases have a homogeneous composition and are in equilibrium throughout the system; (2) fractional equilibrium crystallisation, where all phases apart from garnet are homogeneous and in equilibrium throughout the system. In the case of garnet, only the outermost rim of the crystal is assumed to be in equilibrium with all other phases, whereas previously formed garnet cores are assumed to be isolated from the system; (3) fractional disequilibrium crystallisation; all phases but garnet are homogeneous and in equilibrium with the entire system. Garnet edges are in equilibrium with all other phases, but the amount of certain elements in equilibrium with this edge is independently controlled to model constrained nutrient availability at the garnet surface.

To model zonation patterns, we divided a P–T interval of interest into regularly spaced P–T points, at each of which we calculated the stable mineral parageneses, modal amounts and compositions of stable phases in the chemical system. The P–T interval between two calculated points is referred to as a P–T increment in the following. The moles of garnet produced over a P–T increment are converted into a volume and a radial growth increment. Garnet composition is then plotted as a garnet zonation pattern by assuming a spherical grain shape. Modelling fractional crystallisation involved modifying the chemical composition of the matrix between two calculated points by removing the amount of each component incorporated in garnet from the bulk rock composition, provided that garnet forms a stable phase in the assemblage. Further, we considered the effect of devolatilisation on the garnet zonation pattern by progressively removing free water from the system in all calculations. For simplicity we did not consider relaxation of the growth zonation patterns due to volume diffusion. In our calculations, we focus on garnet growth in a rock with average mid-ocean ridge basalt (MORB) composition (Schilling et al. 1983) along a typical, subduction-type, HP metamorphic path.

Implications for transport-controlled garnet growth

Thermodynamic phase equilibrium requires that mineral nutrients be homogeneously available at any point in the rock to enable equilibrium phase transitions. But there is ample evidence that this situation is usually not attained in metamorphic rocks (Carlson 1989; Dohmen et al. 2003; Dohmen and Chakraborty 2003). In our models, we assume the simple case in which intercrystalline element transport is sluggish and rapid mineral crystallisation leads to small-scale chemical inhomogeneities around porphyroblasts.

Figure 1 shows such a possible relative concentration gradient caused by limited supply of a certain element in the matrix around a garnet porphyroblast. We further

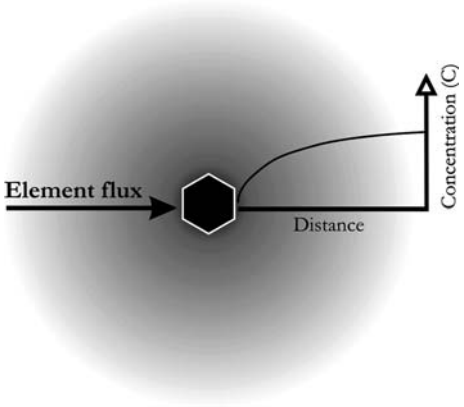

Fig. 1 Simplified illustration of a possible relative concentration gradient around a garnet porphyroblast. In this case, the element concentration at the garnet edge is controlled by the element flux towards the surface, rather than by chemical equilibrium with other phases

assume that the amount of an element incorporated in the garnet edge is not controlled by equilibrium with all other phases but by the nutrient-availability. This is in turn dependent on the flux of these nutrients towards the garnet surface. In the absence of appropriate data for intercrystalline diffusion coefficients for the considered elements and without a quantitative estimate for the concentration gradient around garnet porphyroblasts, we modelled simple, time-independent and distance-independent end-member cases:

1. The amount of the transport-controlled garnet nutrient, available for the garnet surface is constant, but lower than the amount predicted by calculations assuming fractional equilibrium crystallisation,
2. at initial garnet growth the amount is higher than calculated in the equilibrium case, but decreases steadily.

The first case allows one to study garnet growth limited by sluggish element transport towards the garnet surface, whereas the second case simulates preferred garnet nucleation in a site where the growth-controlling element is enriched, but sluggish element transport and fractional crystallisation cause rapidly decreasing concentration of the transport-controlled element in the matrix around the garnet porphyroblast.

Modelling of transport-controlled garnet growth

Modelling transport-controlled garnet crystallisation with Gibbs energy minimisation methods requires that the incorporation of certain elements into the garnet solid solution is independent from the thermodynamic equilibrium in the entire rock. To take this boundary condition into account, we controlled the amount of a specific element available for the garnet surface independent of global equilibrium. THERIAK-DOMINO uses the model of endmembers to construct the Gibbs energy versus composition (G–X) curves of multicomponent solid solutions. In the case of garnet, the endmembers of the solid solution are Grossular ($Ca_3Al_2Si_4O_{12}$), Almandine ($Fe_3Al_2Si_4O_{12}$), Pyrope ($Mg_3Al_2Si_4O_{12}$) and Spessartine ($Mn_3Al_2Si_4O_{12}$). To model transport-controlled element incorporation into the garnet solid solution, we replaced a specific endmember of the garnet solid solution with one that has the same thermodynamic properties as the replaced endmember, but is defined by a substitute-element (SE) that has equal weight and charge as the replaced element and is only incorporated into garnet and the SE-oxide. As long as the SE-oxide does not form a stable phase, any amount of SE added to the system is incorporated into the garnet solid solution, which enables us to independently control the amount of that specific element available for the garnet edge. To model a flux that controls the availability of the transport-controlled element we defined the amount of the substitute element available for the garnet edge at every calculated step. Because our models are time-independent the amount of the substitute element per calculated step is referred to as "nutrient availability". To maintain a closed system an amount of the replaced element equal to that of the added substitute element is subtracted from the bulk composition. The thermodynamic implications of that model, as well as a short description of the calculation routine are given in the Appendix 1.

Fig. 2 shows the modelled amount of calcium incorporated in the garnet edge at every calculated step assuming fractional equilibrium crystallisation (bold curve) . The two other curves display the amount of the Ca-substitute in the garnet edge at every calculated step for the two different disequilibrium crystallisation scenarios . We controlled the amounts of manganese, calcium and aluminium that are incorporated at every calculated step. This is because garnet stability at lower temperatures is controlled by the manganese content in the bulk rock composition (Ganguly 1968; Loomis and Nimick 1982, Droop and Harte 1995, Mahar et al. 1997). Therefore, garnet growth is strongly dependent

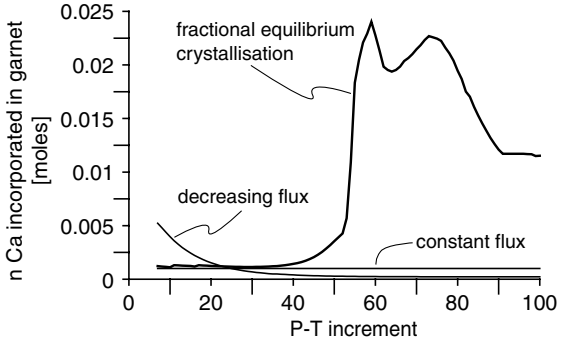

Fig. 2 Amount of calcium incorporated in the garnet edge at every calculated step. The bold curve shows the incorporated Ca-amount calculated for fractional equilibrium crystallisation, the two other curves display the limited amount available for the garnet edge for the two different disequilibrium crystallisation scenarios (see text)

on the amount of manganese available for the garnet crystal. Calcium and aluminium nutrient availabilities are also specified because there is ample evidence for diffusion-controlled garnet growth due to sluggish intercrystalline transport of calcium and aluminium in amphibolite-facies metapelitic schists (Chernoff and Carlson 1997; Spear and Daniel 2001).

Results

Garnet composition for the average MORB chemistry in the water-saturated and quartz-saturated model system Na + Ca + K + Fe + Mg + Al + Si + H + O + Mn (NCKFMASHOMn) is shown in Fig. 3 a–e. Also shown are the zero mode lines for the minerals that have the strongest influence on garnet composition with respect to a certain element. Due to large uncertainties in solid solution models and standard state data (e.g., amphiboles), the pressures and temperatures in the diagram should be taken as approximate values. Nevertheless, the calculated phase relations match the mineral parageneses commonly observed in HP metamorphic rocks. At lower temperatures the garnet-free assemblages comprise chlorite, epidote, phengite, ± paragonite, ± feldspar and/or omphacite. With increasing pressure and temperature, calcic and sodic amphibole, lawsonite and garnet become stable and paragonite disappears. Thus, the modelled phase relations are typical of epidote- and/or lawsonite-bearing, blueschist-facies assemblages. At eclogite-facies conditions, lawsonite, calcic and sodic amphibole disappear and the stable paragenesis is garnet + omphacite + phengite ± kyanite and epidote. The arrow in Fig. 3a shows the P–T interval within which garnet growth is modelled. The P–T interval starts at 375°C and 8 kbar, ends at 650°C/28 kbar and was divided into 100 calculation points, which results in a Δ(P,T) of 0.2 kbars and 2.75°C for each increment.

The isopleth pattern for garnet mode (Fig. 3a) shows three growth stages along the considered P–T interval, each of which is indicated by changing distance between the isopleths. At lower temperatures garnet abundance is very low and garnet growth is controlled by the equilibrium with chlorite. The spacing between the isopleths decreases rapidly near the zero mode line of chlorite, indicating increasing growth rate with increasing temperature. Above chlorite stability, garnet growth is controlled by the consumption

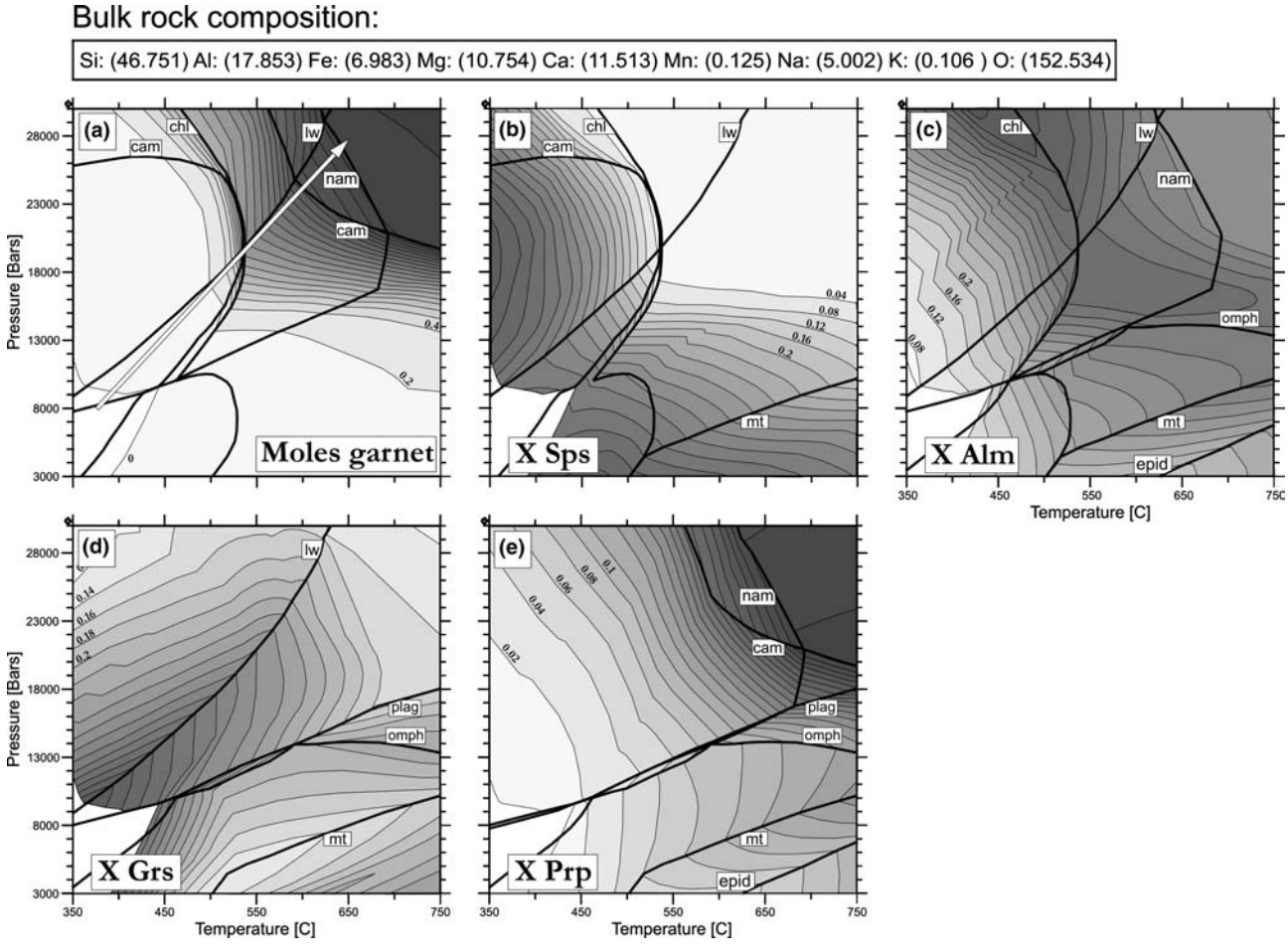

Fig. 3 Garnet mode (**a**), composition (**b**—**e**) and mineral isograds most influencing garnet composition for an average basaltic rock in the water saturated NCKFMASHOMn system. Darker colours display higher mole fractions. The arrow marks the P–T segment along which garnet evolution is modelled

of calcic amphibole (between 530 and 600°C) and sodic amphibole (above 600°C). At eclogite-facies conditions, garnet growth decreases as indicated by the rapid increase of isopleth spacing. The spessartine isopleths (Fig. 3b) are parallel to those for the garnet mode, reflecting the dependence of garnet growth on the partitioning of manganese between garnet and chlorite at lower temperatures. The contours of almandine and grossular (Fig. 3c and d) are very arcuate and much more influenced by the changing mineral parageneses. Almandine shows a saddle-like maximum that separates low-grade and medium-grade garnets with increasing almandine content from high-pressure garnets with decreasing almandine content. Grossular isopleths (Fig. 3d) show a very complex pattern below the omphacite stability, caused by the presence of Ca-bearing plagioclase. At higher pressures, lawsonite has the strongest influence on the grossular contours. The zero mode line of lawsonite strongly deflects the isopleths and forms the crest of a ridge-like grossular maximum. Although the isopleths are highly arcuate, grossular content of garnet decreases steadily towards higher pressures and temperatures. Pyrope isopleths (Fig. 3e) are very regular at higher pressures and are most deflected at the zero mode line of sodic amphibole at the transition to the eclogite field.

Of course, we must keep in mind that these two-dimensional equilibrium diagrams are only valid if all stable phases are in equilibrium and no isolated mineral cores exist. They are inadequate if we consider fractional crystallisation during metamorphism, because then the chemical equilibrium is a path-dependent function. Therefore, the isopleths in Fig. 3 that are calculated for homogeneous crystallisation yield only an approximation of the garnet composition in the case of fractional crystallisation.

Homogeneous and fractional equilibrium crystallisation

The diagrams in Fig. 4 show a comparison of the abundance of newly formed garnet and other minerals as well as the resulting zonation pattern for homogeneous and fractional equilibrium garnet crystallisation along the considered P–T interval. We refer to the amount of newly formed garnet per P–T increment as the growth increment. Fractional garnet crystallisation has a major influence on the garnet growth increment. The plots in Fig. 4a show the garnet growth stages for homogeneous crystallisation caused by the different garnet-producing reactions described above. For fractional crystallisation, the growth increment is constant after initial garnet formation but the increase in growth increment at chlorite breakdown is much more pronounced. After this first growth stage, the growth increment decreases abruptly and becomes more or less constant up to eclogite facies conditions.

The plots in Fig. 4b show that fractional crystallisation influences the mineral paragenesis. The stability fields of lawsonite and sodic amphibole are enlarged by fractional crystallisation. Lawsonite becomes stable at upper greenschist and blueschist-facies conditions and sodic amphibole is stable at eclogite-facies conditions (Fig. 4b). The compositional trend in the resulting zonation patterns is similar. Both patterns have a spessartine-rich and grossular-rich core and a pyrope-rich and almandine-rich rim, a commonly observed zonation pattern in medium-pressure and high-pressure rocks. Fractional crystallisation is responsible for the plateau-like pattern of all components between core and rim compositions and causes a drastic increase in pyrope content at the outermost rim.

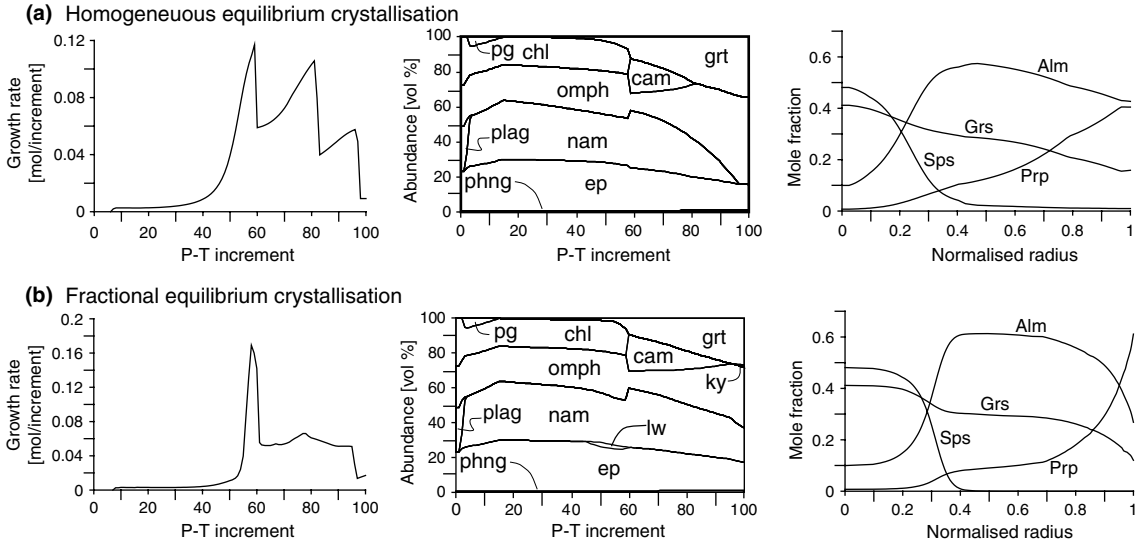

Fig. 4 Garnet growth increments, mineral abundances and modelled garnet zonation patterns for **a** homogeneous and **b** fractional equilibrium crystallisation along the P–T segment shown in Fig. 2a. The step-like garnet growth in **a** is caused by progressive consumption of chlorite, calcic and sodic amphibole

Fractional disequilibrium crystallisation

Disequilibrium incorporation of manganese

Figure 5 shows the calculated growth increment (Fig. 5a) and the resulting zonation pattern (Fig. 5b) for garnet growth with constant manganese availability to the garnet surface. Comparison of these diagrams with those calculated for fractional equilibrium crystallisation shows interesting differences. In both cases the growth increment increases slightly after initial garnet formation and increases rapidly at chlorite breakdown. The position of the peak marking the breakdown of chlorite is shifted towards lower pressures and temperatures in calculations with transport-controlled element incorporation. The rapid decrease in growth increment at the transition to the eclogite facies, caused by the consumption of sodic amphibole, occurs at lower metamorphic conditions. Apart from a small rise in spessartine content at the outermost rim of the resulting zonation pattern, the calculated core-to-rim zonations show no significant differences.

The diagrams in Fig. 6 are calculated for a decreasing availability of manganese at the garnet surface. Decreasing manganese availability has a significant influence on the garnet growth increment (Fig. 6a) and the resulting zonation pattern (Fig. 6b). In contrast to fractional equilibrium garnet crystallisation, the growth increment at decreasing manganese availability decreases steadily after initial garnet formation until the rise near the P–T increment 50. This potentially leads to a complete interruption of garnet growth at lower pressures and temperatures. The lowest garnet production occurs near the steepest compositional gradient. At conditions above chlorite stability, garnet growth is independent of manganese availability. Although the compositional trend of all garnet components in the zonation pattern remains unchanged, decreasing growth increment combined with compositional changes in garnet cause compositional plateaus in the growth patterns at conditions with high garnet production. Steep compositional gradients result when only little garnet is produced (Fig. 6b). Abrupt compositional changes in the resulting zonation pattern occur when garnet growth decreases rapidly or is interrupted.

Disequilibrium incorporation of calcium

Figure 7 shows the growth increment (Fig. 7a) and calculated zonation pattern (Fig. 7b) for constant calcium availability to the garnet edge. The growth increment at lower pressures and temperatures shows the same trend as for the equilibrium calculations, but disequilibrium incorporation of calcium enlarges the stability field of chlorite. The increase in garnet growth increment caused by the breakdown of chlorite is shifted towards higher pressure-conditions and temperature-conditions (Fig. 7a). The second increase of growth increment caused by the consumption of sodic amphibole is more pronounced in the disequilibrium growth model. The calculated zonation patterns differ significantly for equilibrium and disequilibrium incorporation of calcium (Fig. 7b). Whereas in the equilibrium calculations grossular content decreases steadily, disequilibrium incorporation of calcium leads to a temporary rise in the Ca component and a significant decrease in Ca towards the garnet rim. The patterns of the other garnet components are not significantly influenced by disequilibrium incorporation of calcium at constant nutrient availability.

The plots in Fig. 8 are calculated for decreasing calcium availability for the garnet edge. In contrast to equilibrium calculations and those assuming constant calcium availability, garnet growth decreases repeatedly in these calculations (Fig. 8a). After initial garnet formation, the growth increment decreases steadily and starts to rise when chlorite stability is reached. Between P and T increment 62 and 65 garnet growth is again interrupted due to the limited calcium supply. After the breakdown of chlorite, the growth increment curve is similar to that calculated for constant nutrient availability. The resulting zonation pattern (Fig. 8b) shows a pronounced increase in grossular and, in addition, an intervening rise in the spessartine component at the transition between core and rim. This leads to a characteristic zonation pattern near the compositional break. As for the disequilibrium incorporation of manganese, repeated growth minima lead to an abrupt compositional transition between core and rim.

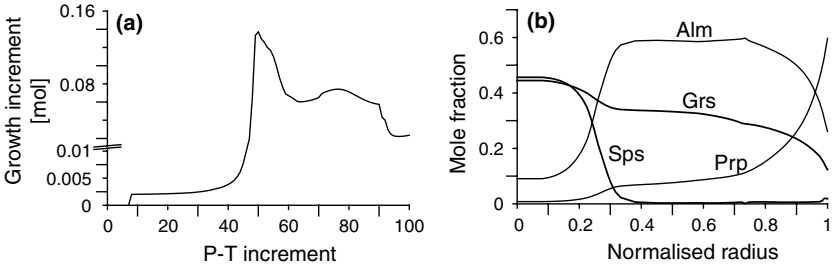

Fig. 5 Garnet growth increment (**a**) and calculated zonation pattern (**b**) for growth along the P–T segment assuming constant manganese availability for the garnet surface. The peak in **a** resulting from chlorite consumption is shifted, compared to calculations assuming equilibrium crystallisation, indicating the influence of disequilibrium garnet growth on the mineral assemblage

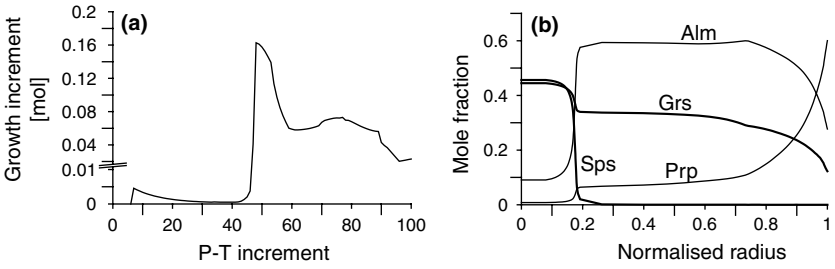

Fig. 6 Garnet growth increment (**a**) and calculated zonation pattern (**b**) for growth along the P–T segment assuming decreasing manganese availability for the garnet surface. Note the decreasing growth increment between initial garnet formation and the peak near point 50. The calculated zonation pattern shows steep compositional gradients caused by limited garnet growth due to disequilibrium element incorporation

Disequilibrium incorporation of aluminium

Because aluminium is incorporated into all four garnet endmembers, the growth increment of garnet is proportional to the amount of aluminium available for the garnet surface. Therefore, limited Al availability will directly control the amount of garnet produced over each P–T increment, because hindered growth of a specific endmember due to limited nutrient availability, cannot be compensated by any other endmember component. This relationship is displayed by the growth increment shown in Fig. 9a, which is calculated for a constant Al availability for the garnet surface. Interestingly, in contrast to Mn and Ca, limited Al availability strongly influences the garnet composition even at higher pressures and temperatures (Fig. 9b).

Although grossular and spessartine components show the same trend as in the models assuming transport-controlled Ca-incorporation and Mn-incorporation, the remarkable pyrope-increase at the garnet rim observed in all other calculations is missing in the models assuming transport-controlled Al incorporation. In the calculations with decreasing Al availability, the growth increment decreases steadily (Fig. 10a) and grossular-rich and spessartine-rich garnet forms almost the entire grain, because the amount of garnet produced at higher pressures is limited by the decreasing nutrient availability. This causes very little almandine-rich and pyrope-rich garnet growth at the outermost rim (Fig. 10b).

Examples from natural rocks

In order to test the validity of our modelled results for natural garnets, we discuss two examples of garnets in high-pressure and medium-pressure metamorphic rocks. The first is an ultra-high-pressure (UHP) eclogite from the Tso Morari area in the Western Himalayas, and the second comes from a medium pressure metapelite from Stuckless Cove, Newfoundland. The latter was intensively investigated by Vance and O'Nions (1990).

Compositional maps of two coalesced garnet grains in the Himalayan sample are shown in Fig. 11a. The maps of iron and manganese show the core of a large grain in the upper left corner and a smaller one on the right side. The core to rim profile 1 in Fig. 11b represents the zonation pattern of the larger grain along the line labelled 1 in Fig. 11a. This profile is clearly different at the margin to that for the overgrowth in the smaller grain (profile 2 Fig. 11b). The volume of the overgrowth is significantly different in different parts of the garnet and the transition between core and rim is less sharp in the larger grain. The zonation pattern of profile 1 is typical of continuous growth, whereas the abrupt compositional break in the pattern of the smaller grain indicates periodic growth with growth interruption. This growth interruption in the smaller grain is most obvious in the grossular and pyrope zonation patterns. At the rim of the larger grain the grossular content decreases continuously from 0.32 to 0.1. In contrast, the continuous decrease in calcium is not recorded in the smaller grain and the grossular fraction decreases abruptly from 0.32 to 0.12. The same difference is observed in the

Fig. 7 Garnet growth increment (**a**) and calculated zonation pattern (**b**) for growth along the P–T segment assuming constant calcium availability for the garnet surface. Disequilibrium incorporation of calcium enlarges the stability field of chlorite (shifted peak in **a**) and causes a characteristic intervening increase in grossular content in the calculated zonation pattern (**b**)

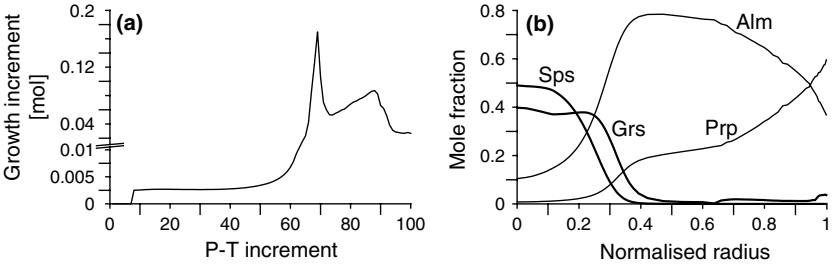

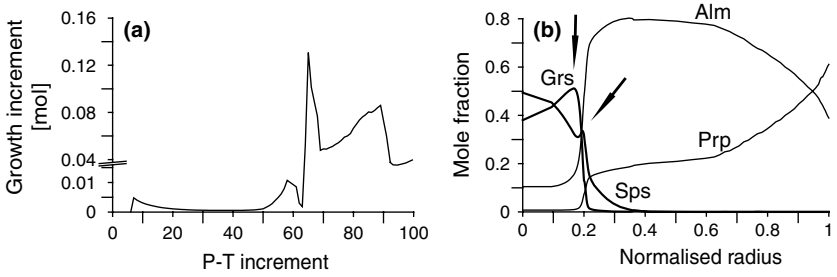

Fig. 8 Garnet growth increment (**a**) and calculated zonation pattern (**b**) for growth along the P–T segment assuming decreasing calcium availability for the garnet surface. Limited calcium supply leads to repeated decrease in growth increment and a characteristic rise in grossular accompanied by an intermediate rise in spessartine components (*arrows* in b)

pyrope content, which rises continuously from 0.02 to 0.25 in the larger grain, but increases in a step-like pattern in the smaller grain. Interestingly, changes in the almandine component are recorded in both grains.

The Stuckless Cove example is similar. Figure 12 shows two zonation patterns from large euhedral garnets in the same hand specimen. Both garnets were separated from the specimen prior to cutting and cut through their centres (D. Vance, personal communication). The isotopic investigations of Vance and O'Nions (1990) showed that the ages of the cores and the rims of these garnets are identical within error, suggesting growth of the entire grain during one metamorphic event. As in the previous example above, one garnet (garnet 2) shows a smooth zonation pattern indicating continuous growth and a complete compositional record, whereas the other grain (garnet 1) has steep compositional gradients in the zonation pattern, which are diagnostic of discontinuous growth. In contrast to grain 2, garnet 1 shows increasing grossular content accompanied by a decreasing almandine component in the core. Near the compositional break, both grains from Newfoundland show an abrupt increase in the spessartine component (arrows in Fig. 12).

Fig. 9 Garnet growth increment (**a**) and calculated zonation pattern (**b**) for growth along the P–T segment assuming constant aluminium availability. In this case garnet growth is directly related to the amount of Al available for the garnet surface. The resulting zonation pattern **b** does not show the strong increase in pyrope content accompanied by a decrease in the almandine component at high-pressures

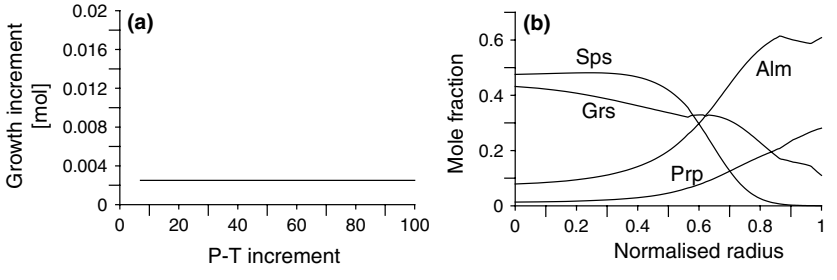

Discussion

The results of our calculations depend strongly on the thermodynamic database, so we tested for the influence of changes in standard state data and solution models. Changing the thermodynamic data shows that although the modifications of standard state data or solid solution formulations do influence the absolute compositions of the phases, they have only minor influence on garnet growth increment and on the shape of the modelled zonation patterns.

Our numerical models support the following conclusions:

1. The incorporation of elements at disequilibrium conditions influences growth increment and garnet composition, leading to different zonation patterns for equilibrium-controlled and diffusion-controlled garnet growth.
2. both smooth and abrupt compositional gradients caused by transport-controlled incorporation of elements in natural garnets can be observed in one and the same sample (Figs. 11 and 12). This reflects small-scale chemical disequilibrium in these rocks.

Zonation patterns indicative of diffusion-controlled garnet growth

Evidence for disequilibrium garnet growth due to small-scale variations in matrix chemistry is given in Chernoff and Carlson (1997) and Spear and Daniel (2001). Chernoff and Carlson (1997) give examples of garnet growth controlled by intercrystalline diffusion in pelitic schists from the Pecuris range, New Mexico. Spear and Daniels (2001) investigated garnets from pelitic schists from Harpswell Neck, Maine. In both studies, fractional crystallisation of garnet led to the development of halos

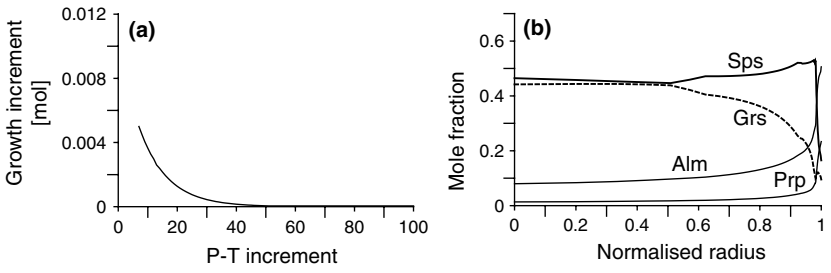

Fig. 10 Garnet growth increment (**a**) and calculated zonation pattern (**b**) for growth along the P–T segment assuming decreasing aluminium availability. Due to the rapidly decreasing growth increment, the compositional break occurs only at the outermost rim **b**

of a chemically depleted matrix or chemical gradients in the intergranular fluid around a growing garnet crystal. These chemical inhomogeneities caused disequilibrium incorporation of calcium in the garnet porphyroblasts.

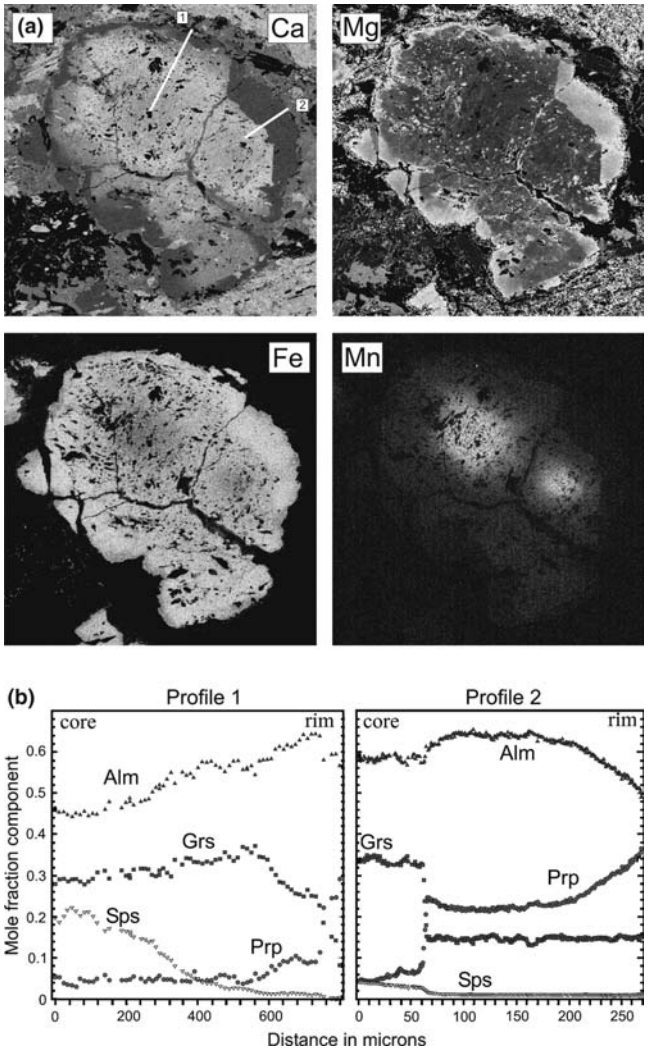

Fig. 11 Compositional mapping (**a**) and compositional profiles (**b**) of a garnet aggregate from the Tso Morari area (Western Himalayas). **a** The Fe-maps and Mn-maps show that the garnet is a composite of two amalgamated grains. The *lines* mark the position of the profiles (1, 2) in Fig. 7b. Profile 1 shows a continuous compositional gradient, whereas profile 2 shows a discrete compositional change at the interface of the core and rim (see text)

The incorporation of calcium in garnets growing in such a depleted zone is assumed to be controlled by element flux rather than by chemical equilibrium between garnet and all other matrix phases. The authors of both papers describe a sudden rise in the grossular content that cannot be related to a metamorphic event that affected the entire rock (Fig. 13).

Our numerical calculations that assume transport-controlled incorporation of calcium in garnet show the same irregular behaviour of calcium as described in the papers above (Figs. 7b, 8b). Depending on nutrient availability, both grossular and spessartine contents rise irregularly at the outer garnet core. Evidence for the incorporation of calcium under disequilibrium conditions is also recorded in the Newfoundland sample of Vance and O'Nions (1990) (Fig. 12). Here too, the

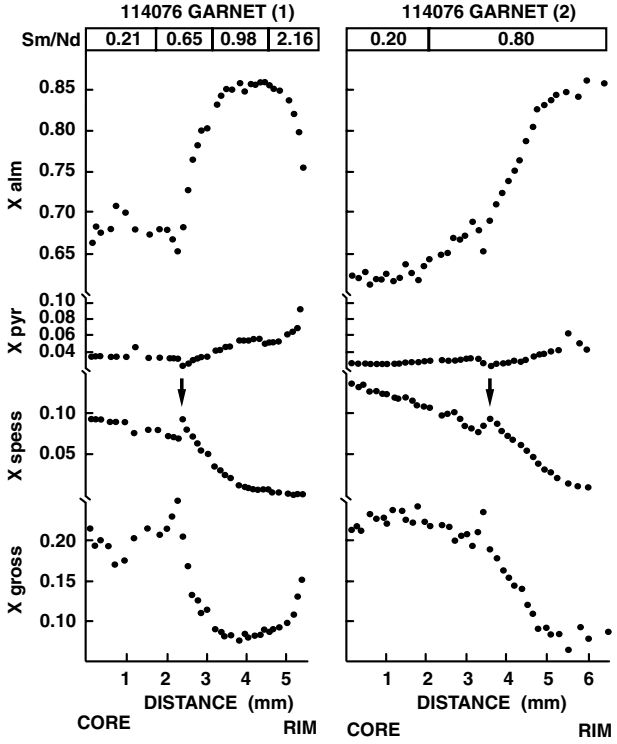

Fig. 12 Compositional profiles across two garnet megacrysts from Stuckless Cove (Newfoundland) (Vance and O'Nions 1990). Garnet 1 shows a marked compositional break between core and rim, which is not visible in garnet 2. Both profiles show an increase in Ca and Mn, which coincides with the compositional break in garnet 1 (*arrows*). See text for discussion

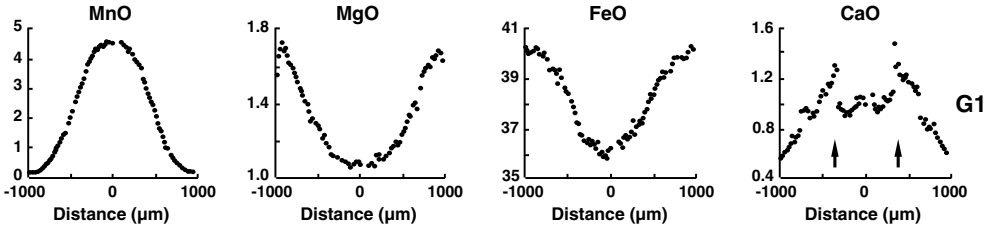

Fig. 13 Compositional profile across a garnet crystal from Pecuris Range, New Mexico, USA (redrawn after Chernoff and Carlson 1997). Note the sudden rise of CaO due to disequilibrium incorporation of calcium (*arrows*)

different zonation patterns for grossular in garnets from the same sample, together with a rise in the spessartine content, can be modelled by assuming transport-controlled incorporation of calcium (Fig. 8). The consistency of modelled and natural garnet zonation patterns indicates that the numerical calculations can predict characteristic zonation patterns caused by the incorporation of certain elements under disequilibrium conditions. These patterns can therefore be used to determine the relative velocities of diffusing elements in metamorphic rocks.

Growth interruptions due to limited nutrient supply

The isopleth pattern (Fig. 3) and the modelled garnet growth along the considered P–T interval (Fig. 4) show that garnet growth in HP rocks occurs in two main stages. At greenschist facies conditions, garnet growth is controlled by the equilibrium with chlorite and the partitioning of manganese between chlorite and garnet. A second garnet growth stage starts with the attainment of blueschist-facies, when garnet grows at the expense of calcic and sodic amphibole. These stages are marked by quite different zonation patterns. Garnets grown at the expense of chlorite along a prograde HP metamorphic path show a characteristic grossular-rich and spessartine-rich core, an increase in almandine and pyrope content, and decreasing spessartine and grossular components towards their rims (e.g. Vance and Mahar 1998). Garnets nucleated at higher pressures and temperatures have almandine-rich cores and show a characteristic decrease in almandine and grossular content, together with a strong increase in the pyrope component at the garnet rims (e.g. Compagnoni and Hirajima 2001).

The amount of garnet initially produced at greenschist-facies conditions is small compared with the abundance of garnet at higher pressures (Fig. 4). Slight changes in nutrient supply might cause growth interruptions and enable resorption of pre-existing grains (Figs. 6 and 8). Garnets growing with a continuous nutrient supply have zonation patterns with a smooth transition between the core and rim composition (Fig. 4). Garnet growth controlled by sluggish nutrient transport is recorded by steep compositional gradients in the zonation patterns and, e.g. in case of calcium, in an irregular increase in grossular and spessartine content at the transition between core and rim compositions (Fig. 8). For growth interruption caused by a cessation of element flux, the zonation patterns might even show abrupt compositional changes (Fig. 6). These zones of abrupt changes in garnet composition can be used to quantify the duration of metamorphic events by calculating the diffusional relaxation of the steep compositional gradient. Therefore, it is crucial to understand the mechanisms that cause these growth interruptions.

Mechanisms of growth interruption and resorption of garnet grains are discussed in Miyazaki (1991, 1996), who compared the zonation patterns and crystal size distribution (CSD) of HP garnets. He argued that the zonation pattern and the observed CSD indicate that smaller garnet grains ceased to grow or dissolved, whereas larger grains grew at the expense of smaller ones. Ostwald ripening is inferred to be the primary process controlling garnet growth in HP rocks (see also Carlson, 1999 and discussion in Carlson, 2000 and Miyazaki, 2000). Yet, Ostwald ripening depends on the surface energy and the volume-to-surface ratio of the garnet grains. It might therefore only play a role at the onset of garnet growth, when small nuclei are unstable and are resorbed. It is very unlikely to affect larger grains at higher metamorphic conditions. Our results show that growth interruptions affecting larger garnet grains, as in the UHP metamorphic garnets from the Himalayan sample, are the result of limited nutrient flux to the garnet surface. But what is the element that controls growth? Our calculations show that manganese-availability and calcium-availability both potentially limit growth at greenschist-facies conditions (Figs. 6 and 8). Manganese stabilizes garnet towards lower temperatures and the absence of a manganese flux strongly affects the garnet growth increment. Calcium is assumed to have slower intercrystalline diffusion velocities and, although grain boundary diffusion velocities for calcium are unknown, for kinetic reasons it is presumed to control growth at lower temperatures. Additionally, limited calcium incorporation in garnet can be easily balanced by changing the compositions and amounts of other pre-existing Ca-bearing phases, such as epidote and calcic amphibole, which might compensate limited garnet growth. Our calculations show that limited supply of both elements might cause growth interruptions at the transition from greenschist-facies to blueschist-facies conditions. In contrast to manganese, the lack of a calcium supply causes characteristic changes in the garnet zonation pattern, such as increasing grossular and spessartine contents. Although there is a slight increase in grossular content in the Himalayan sample (Fig. 11b), there is no increase in spessartine content, which we take

as evidence that the growth interruption observed in the smaller grain in the UHP eclogite is caused by the limited availability of manganese. This requires very short equilibration distances for this element and suggests very slow element diffusivities in that rock. Recent publications have shown very short equilibration distances for manganese (Hirsch et al. 2003), which suggests that small-scale chemical disequilibrium even of rapidly diffusing elements might be a common phenomenon in metamorphic rocks.

Possible misinterpretation due to non-central cutting planes

Figure 14 shows a textural relation of the two Himalayan garnets that might possibly lead to a misinterpretation of the observed zonation patterns. The transition zone between core and rim composition in the smaller grain is about 10 μm wide, whereas in the larger grain this transition occurs across a distance of more than 200 μm (Fig. 11b). If in both grains this zone is not more than 10 μm wide this would require a cutting angle of more than 87° in the larger grain (Fig. 14). Consequently the larger grain must be about 3.2 cm in diameter, which is more than ten times larger than the observed garnet grain size in this sample. Therefore there is no reason to believe that the difference between the zonation patterns is the result of a non-central cutting plane.

Of course our interpretation assumes garnet growth during a single metamorphic event. Although in contrast to the Stuckless Cove sample, this cannot be proved by geochronological data in the Himalayan sample, the correlation of the observed compositional trends in the natural garnets with those calculated for a UHP metamorphic path clearly suggests that cores and rims of the Himalayan garnets grew during a single UHP metamorphic event.

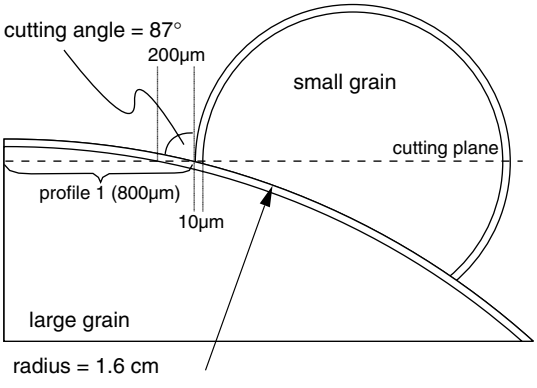

Fig. 14 Schematic illustration of a textural relation between the two garnets in Fig. 11, that might possibly lead to a misinterpretation of the observed compositional profiles (see text for discussion)

Evidence for small-scale chemical variations in metamorphic rocks

The calculations above show that disequilibrium element incorporation of manganese, calcium and aluminium leads to distinct garnet zonation patterns. Zonation patterns diagnostic for disequilibrium incorporation of elements as well as for fractional equilibrium crystallisation can be observed in one sample (Figs. 11, 12). The occurrence of both steep and smooth zonation patterns in garnets from the same sample and with similar grain sizes precludes the possibility that the differences in the zonation patterns are the result of relaxation due to intracrystalline diffusion, because volume diffusion would affect all garnets to the same extent. This supports the idea that intercrystalline diffusional transport of the garnet nutrients and therefore, the amount by which the matrix around garnet is depleted, differs within small spatial domains in metamorphic rocks. Pre-existing inhomogeneities, such as foliations or chemical layering, might additionally influence element transport and favour disequilibrium garnet growth. The calculations also show that disequilibrium garnet growth significantly influences phase equilibria (Figs. 4, 7). The incorporation of elements at disequilibrium, e.g. calcium, has a significant influence on thermobarometric estimates. Disregarding these effects can lead one to misinterpret garnet zonation patterns and calculated phase equilibrium diagrams, resulting in erroneous P–T paths. Disequilibrium garnet growth seems to be common in metamorphic rocks and has been generally overlooked so far. Although further investigations are necessary to infer more precisely the growth kinetics of these samples, the examples show that the effects modelled in our calculations are observed in natural samples. Considered together, the spatial distribution of garnet grains, their zonation patterns, their trace element zonations and numerical growth models of garnet zonation patterns yield information about the processes limiting garnet growth such as intercrystalline element transport or dissolution of pre-existing grains.

Conclusions

Numerical calculations show that fractional crystallisation of garnet changes the chemistry of the matrix around garnet porphyroblasts. These changes have a strong influence on garnet growth in high-pressure rocks. Fractional crystallisation together with sluggish intercrystalline diffusion velocities leads to chemically depleted zones around porphyroblasts. Garnet growth in such depleted zones is controlled by elemental flux rather than by chemical equilibrium with the matrix phases. Diffusion-controlled garnet growth is often recorded in typical garnet zonation patterns. Numerical models of diffusion-controlled elemental incorporation in garnet show that limited manganese and/or calcium transport leads to characteristic garnet zonation pattern

with steep compositional gradients and an intervening rise in grossular and spessartine components. It might cause growth interruptions at the transition from greenschist to blueschist facies. In contrast, garnets in equilibrium with matrix phases grow homogeneously and therefore have shallower compositional gradients. The modelled zonation patterns are in good agreement with those observed in natural garnets with a diffusion-controlled growth history. The observation of both types of garnet zonation patterns within small spatial domains in the same sample indicates compositional variations in the matrix or the intercrystalline fluid locally distributed in the matrix. Furthermore, phase relations in calculations assuming diffusion-controlled garnet growth differ significantly from those assuming fractional and homogeneous equilibrium crystallisation. This might lead to erroneous interpretations of thermodynamically calculated phase relations. Therefore, the spatial distribution of garnet grains and their zonation patterns, considered together with numerical growth models of garnet zonation patterns yield information about the processes limiting garnet growth. These include intercrystalline element transport or dissolution of pre-existing grains. Further, the interpretation of the modelled zonation patterns yield better insights into the P–T evolution of HP rocks despite obvious disequilibrium on a whole-rock scale.

Acknowledgements We thank Lukas Baumgartner (Lausanne) for numerous helpful suggestions, Claudio Rosenberg for his comments on the manuscript as well as David Hirsch and Jibamitra Ganguly for very helpful reviews that significantly improved the manuscript. The project was supported by German Science Foundation (DFG) grant HA 2403/5.

Appendix 1

Calculation routine

The algorithm of THERIAK calculates the stable mineral assemblage by minimising the Gibbs free energy in a multicomponent system with fixed bulk rock composition. This is done by several steps including linear and non-linear programming problems. In the first step THERIAK searches each solution phase for the composition with the lowest Gibbs energy of formation ($\Delta_f G$) in the system. The solid solution phases are defined by endmembers, i.e. each solution is considered to be made of any number of species, where each of these species is a valid endmember. $\Delta_f G$ of the solid solutions is defined by the Gibbs-Duhem equation:

$$\Delta_f G = \sum_{j=1}^{ne} xj \cdot \mu j,$$

with: *ne* is the number of endmembers in the solution phase, μ_j the chemical potential of endmember *j* in the solution phase, x_j is the concentration of endmember *j* in the solution phase and $\mu_j = \mu_j^0 + \alpha \cdot R \cdot T \cdot \ln(aj)$, where μ_j^0 is the chemical potential of pure endmember *j*, α the site occupancy integer, *R* the Gas constant, *T* the temperature and a_j is the activity of component *j* in the solution phase.

The solid solution models and Margules parameters used to determine $\Delta_f G$ are given in the Appendix 2. The compositions with the smallest $\Delta_f G$ are added to the database as phases with fixed composition.

In the second step THERIAK determines the mineral assemblage with the lowest Gibbs free energy. This problem can be formulated as:

$$\text{minimise } G = \sum_{k=1}^{N} nk \cdot gk,$$

where n_k is the number of moles, g_k the molar Gibbs free energy of phase *k* and *N* is the number of coexisting phases in the system. Details of the algorithm are described in de Capitani and Brown (1987).

Calculation procedure for diffusion-controlled garnet growth

Modelling diffusion-controlled garnet growth with the method described above requires that at least one element of the garnet solid solution is independent of the global equilibrium. To model this condition we replaced an endmember of the garnet solid solution with one that has the same thermodynamic properties as the replaced endmember, but is defined by a substitute element (SE) not incorporated into other phases in the system. The thermodynamic implications of that model are displayed by the G–X diagrams in Fig. 15. Three G–X binaries are influenced by our constraints. In the binary between SE and the replaced element (RE), all phases are endmembers, garnet and the SE-oxide being the only phases with a SE-endmember. In the binaries between SE and any other element (Y), garnet forms a solid solution and all other minerals are endmembers.

In the binaries between RE and all other elements (Y), garnet is an endmember phase of Y, whereas other phases (A and B) may form solid solutions. The tangent points of the shaded planes to the G–X curves in Fig. 15, that display possible hyperplanes, calculated by the THERIAK-DOMINO algorithm, represent the stable mineral assemblages. In case of the bulk rock composition X_{sys1} the stable assemblage is $B_{ss1} + A_{ss} + Grt_{ss1}$. Changing amounts of SE in the system, e.g. due to fractional garnet crystallisation or insufficient nutrient supply, may have consequences for phases not containing SE because the tangent point of the hyperplane to the garnet solid solution changes and the new hyperplane might not touch the G–X curves of phase A or B, as demonstrated by the second, more steeply dipping plane, that represents the stable phases for bulk rock composition X_{sys2}. In this case, the stable assemblage is $B_{ss2} + Grt_{ss2}$. In a multicomponent system $\Delta_f G$ and the components define

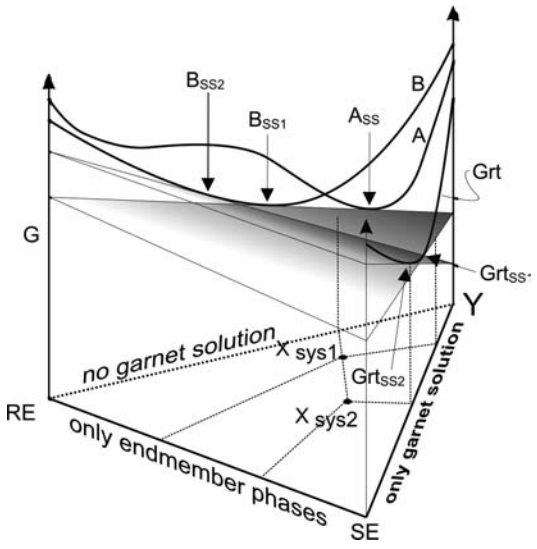

Fig. 15 Schematic G–X relations in the binaries *replaced elements–substitute elements–all other elements* (*RE–SE–Y*). The curved lines display the G–X curves of different minerals (A, B and Grt). The shaded planes display possible hyperplanes that define the mineral assemblage with the lowest Gibbs free energy. Note that changing amounts of SE in the system changes the tangent point of the hyperplane to the G–X curve of garnet and therefore influences the phase relations along other binaries. This is displayed by the second, more steeply dipping plane

a hyperspace and the mineral assemblage with the lowest $\Delta_f G$ is defined by a hyperplane that is tangent to the $\Delta_f G$ curves of the (stable) phases.

Appendix 2

Solid solution endmembers and Margules Parameters

Garnet

In the models we used the solid solution formulation of Ganguly et al. 1996. A comparison of the results with those calculated with the Berman 1990 formulation showed no significant differences in the garnet zonation patterns.

Endmembers: Pyrope, Grossular, Almandine, Spessartine

Ideal 1-site-mixing and Margules-type excess function:

Solid solution models:

1. Ganguly et al. (1996)
2. Berman (1990)

Clinopyroxene

Endmembers: Diopside, Hedenbergite, Jadeite

Ideal 1-site-mixing and Margules-type excess function.

Solid solution model: Meyre et al. (1997)

Sodic amphibole

Endmembers: Glaucophane, Fe-Glaucophane

Ideal 1-site-mixing and Margules-type excess function:

Glaucophane–Fe-Glaucophane	W^H	W^S	W^V
112	10000	0.00	0.00

Phengite

Endmembers: Muscovite, Celadonite, Fe-Celadonite; Pyrophyllite

Ideal 1-site-mixing and Margules-type excess function:

modified from Vidal and Parra (2000)

Muscovite–Celadonite	W^H	W^S	W^V
112	−10500.0	55.0	0.79
Muscovite–Fe-celadonite			
112	−10500.0	15.0	0.78
Muscovite–Pyrophyllite			
112	30000.0	20.0	−0.17
122	30000.0	20.0	−0.17

Chlorite

Two different solution models were tested; we preferred the modified Vidal and Parra (2000) model.

Endmembers: Amesite, Clinochlore, Daphnite, Mn-Chlorite.

Ideal 3-site-mixing and Margules-type excess function:

	W^H	W^S	W^V
(1) Modified from Vidal and Parra (2000)			
Amesite–Clinochlore			
112	−9400	−30	−0.2
Amesite–Daphnite			
112	−12000	35	−0.5
Mn-chlorite–Daphnite			
112	−10000	0	0
(2) Modified from Holland and Powell (1998)			
Amesite–Clinochlore			
112	18000	0	0
Amesite–Daphnite			
112	13500	0	0
Clinochlore–Daphnite			
112	2500	0	0

Calcic Amphibole

Endmembers: Pargasite, Ferropargasite, Tremolite, Ferro-actinolite, Aluminotschermakite, Alumino-ferrotschermakite

Ideal 3-site-mixing and Margules-type excess function:

Modified from Mader et al. (1994)

	W^H	W^S	W^V
Pargasite–Tremolite			
112	9743.68	0	0
Tremolite–Ferro-actinolite			
112	2108.23	0	0
Aluminotschermakite–Tremolite			
112	21431.32	0	0
Alumino-ferrotschermakite–Ferro-actinolite			
112	−15492.29	0	0
Aluminotschermakite–Alumino-ferrotschermakite			
112	2108.23	0	0
Pargasite–Ferropargasite			
112	2108.23	0	0

Biotite

Endmembers: Phlogopite, Eastonite, Annite, ordered Biotite

Ideal 3-site-mixing and Margules-type excess function:

	W^H	W^S	W^V
Phlogopite–Annite			
112	9000.0	0	0
Phlogopite–Eastonite			
112	10000	0	0
Phlogopite–o-Biotite			
112	3000	0	0
Annite–Eastonite			
112	−1000	0	0
Annite–o-Biotite			
112	6000	0	0
Eastonite–o-Biotite			
112	10000	0	0

Feldspar

Endmembers: Albite, Anorthite, K-Feldspar

Ideal 1-site-mixing and Margules-type excess function.

Solid solution model: Furman and Lindsley (1988).

References

Ayres M, Vance D (1997) A comparative study of diffusion profiles in himalayan and dalradian garnets; constraints on diffusion data and the relative duration of the metamorphic events. Contrib Miner Petrol 128:66–80

Berman RG (1990) Mixing properties of Ca–Mg–Fe–Mn garnets. Am Miner 75:328–344

de Capitani C, Brown TH (1987) The computation of chemical equilibrium in complex systems containing non-ideal solutions. Geochim Cosmochim Acta 51:2639–2652

Carlson WD (1989) The Significance of intergranular diffusion to the mechanisms and kinetics of porphyroblast crystallisation. Contrib Miner Petrol 103:1–24

Carlson WD (1991) Competitive diffusion-controlled growth of porphyroblasts. Miner Mag 55:317–330

Carlson WD (1999) The case against Ostwald ripening of porphyroblasts. Can Miner 37:403–413

Carlson WD (2000) The case against Ostwald ripening of porphyroblasts: reply. Can Miner 38:1029–1032

Chernoff CB, Carlson WD (1997) Disequilibrium for Ca during growth of pelitic garnet. J Metamorphic Geol 15:421–438

Compagnoni R, Hirajima T (2001) Superzoned garnets in the coesite-bearing Brossasco-Isasca Unit, Dora-Maira massif, Western Alps, and the origin of the whiteschists. Lithos 57:219–236

Cooke RA, O Brien PJ, Carswell DA (2000) Garnet zoning and the identification of equilibrium mineral compositions in high-pressure–temperature granulites from the Moldanubian Zone, Austria. J Metamorphic Geol 18:551–569

Cygan RT, Lasaga AC (1982) Crystal-growth and the formation of chemical zoning in garnets. Contrib Miner Petrol 79:187–200

Dohmen R, Chakraborty S (2003) Mechanism and kinetics of element and isotopic exchange mediated by a fluid phase. Am Miner 88:1251–1270

Dohmen R, Chakraborty S, Palme H, Rammensee W (2003) Role of element solubility on the kinetics of element partitioning: In situ observations and a thermodynamic kinetic model. J Geophys ResSolid Earth 108:

Droop GTR, Harte B (1995) The effect of Mn on the phase relations of medium-grade pelites; constraints from natural assemblages on petrogenetic grid topology. J Petrol 36:1549–1578

Enami M (1998) Pressure-temperature path of sanbagawa prograde metamorphism deduced from grossular zoning of garnet. J Metamorphic Geol 16:97–106

Escuder-Viruete J, Indares A, Arenas R (2000) P–T paths derived from garnet growth zoning in an extensional setting; an example from the tormes gneiss dome (Iberian Massif, Spain). J Petrol 41:78

Fuhrman ML, Lindsley DH (1988) Ternary-feldspar modeling and thermometry. Am Miner 73:201–215

Ganguly J (1968) Analysis of stabilities of chloritoid and staurolite and some equilibria in system Feo–Al_2O_3–SiO_2–H_2O–O_2. Am J Sci 266:277–298

Ganguly J, Cheng W, Tirone M (1996) Thermodynamics of alumosilicate garnet solid solution: new experimental data, an optimized model, and thermometric applications. Contrib Miner Petrol 126:137–151

Ganguly Y, Chakraborty S, Sharp TG, Rumble D (1996) Constraint on the time scale of biotite-grade metamorphism during Acadian orogeny from a natural garnet–garnet diffusion couple. Am Miner 81:1208–1216

Hirsch DM, Prior DJ, Carlson WD (2003) An overgrowth model to explain multiple, dispersed high-Mn regions in the cores of garnet porphyroblasts. Am Miner 88:131–141

Holland TJB, Powell R (1998) An internally consistent thermodynamic data set for phases of petrological interest. J Metamorphic Geol 16:309–343

Hollister LS (1966) Garnet Zoning - an Interpretation based on rayleigh fractionation model. Science 154:1647–1651

Lasaga AC, Jiang JX (1995) Thermal History of Rocks - P–T-t Paths from Geospeedometry, Petrological Data, and Inverse-Theory Techniques. Am J Sci 295:697–741

Loomis TP (1982) Numerical-simulation of the disequilibrium growth of garnet in chlorite-bearing aluminous pelitic rocks. Can Miner 20:411–423

Loomis TP, Nimick FB (1982) Equilibrium in Mn–Fe–Mg aluminous pelitic compositions and the equilibrium growth of garnet. Can Miner 20:393–410

Mader UK, Percival JA, Berman RG (1994) Thermobarometry of garnet–clinopyroxene-hornblende granulites from the kapuskasing structural zone. Can J Earth Sci 31:1134–1145

Mahar EM, Baker JM, Powell R, Holland TJB, Howell N (1997) The effect of Mn on mineral stability in metapelites. J Metamorphic Geol 15:223–238

Marmo BA, Clarke GL, Powell R (2002) Fractionation of bulk rock composition due to porphyroblast growth: effects on eclogite facies mineral equilibria, Pam Peninsula, New Caledonia. J Metamorphic Geol 20:151–165

Menard T, Spear FS (1993) Metamorphism of calcic pelitic schists, stratford dome, vermont - compositional zoning and reaction history. J Petrol 34:977–1005

Meyre C, de Capitani C, Partzsch JH (1997) A ternary solid solution model for omphacite and its application to geothermobarometry of eclogites from the middle Adula Nappe (Central Alps, Switzerland). J Metamorphic Geol 15:687–700

Miyazaki K (1991) Ostwald ripening of garnet in high P/T metamorphic rocks. Contrib Miner Petrol 108:118–128

Miyazaki K (1996) A numerical simulation of textural evolution due to Ostwald ripening in metamorphic rocks: A case for small amount of volume of dispersed crystals. Geochim Cosmochim Acta 60:277–290

Miyazaki K (2000) The case against Ostwald ripening of porphyroblasts: discussion. Can Miner 38:1027–1028

O'Brien PJ (1999) Asymmetric zoning profiles in garnet from HP to HT granulite and implications for volume and grain-boundary diffusion. Miner Mag 63:227–238

Okudaira T (1996) Temperature-time path for the low-pressure Ryoke metamorphism, Japan, based on chemical zoning in garnet. J Metamorphic Geol 14:427–440

Perchuk A, Philippot P, Erdmer P, Fialin M (1999) Increments of thermal equilibration at the onset of subduction deduced from diffusion modeling of eclogitic garnets, Yukon–Tanana terrane, Canada. Geology 27:531–534

Powell R, Holland T, Worley B (1998) Calculating phase diagrams involving solid solutions via non-linear equations, with examples using THERMOCALC. J Metamorphic Geol 16:577–588

Schilling JG, Zajak M, Evans R, Johnston T, White W, Devine JD, Kingsley R (1983) Pettrologic and geochemical variations along the mid-atlantic ridge from 27°N to 73°N. Am J Sci 283:510–586

Spear FS (1993) Metamorphic phase equilibria and pressure–temperature–time paths. Monograph Mineralogical Society of America, Washington DC

Spear FS, Daniel CG (2001) Diffusion control of garnet growth, Harpswell Neck, Maine, USA. J Metamorphic Geol 19:179–195

Spear FS, Selverstone J (1983) Quantitative P–T path from zoned minerals; theory and tectonic applications. Contrib Miner Petrol 83:348–357

Spear FS, Selverstone J, Hickmott D, Crowley P, Hodges KV (1984) P–T paths from garnet zoning; a new technique for deciphering tectonic processes in crystalline terranes. Geology 12:87–90

Vance D, Mahar E (1998) Pressure–temperature paths from P–T pseudosections and zoned garnets; potential, limitations and examples from the Zanskar Himalaya, NW India. Contrib Miner Petrol 132:225–245

Vance D, O'Nions RK (1990) Isotopic chronometry of zoned garnets—growth kinetics and metamorphic histories. Earth Planet Sci Lett 97:227–240

Vidal O, Parra T (2000) Exhumation paths of high-pressure metapelites obtained from local equilibria for chlorite-phengite assemblages. Geol J 35:139–161

White RW, Powell R, Holland TJB, Worley BA (2000) The effect of TiO2 and Fe2O3 on metapelitic assemblages at greenschist and amphibolite facies conditions; mineral equilibria calculations in the system K2O–FeO–MgO–Al2O3–SiO2–H2–Fe2O3. J Metamorphic Geol 18:497–511

White RW, Powell R, Holland TJB (2001) Calculation of partial melting equilibria in the system Na2O–CaO–K2O–FeO–MgO–Al2O3–SiO2–H2O (NCKFMASH). J Metamorphic Geol 19:139–153

Worley B, Powell R (2000) High-precision relative thermobarometry; theory and a worked example. J Metamorphic Geol 18:91–101